0026-895X/08/7405-1308–1318$20.00
MOLECULAR PHARMACOLOGY
Copyright © 2008 The American Society for Pharmacology and Experimental Therapeutics
Mol Pharmacol 74:1308–1318, 2008

Vol. 74, No. 5
49783/3398852
Printed in U.S.A.

Full Pharmacological Efficacy of a Novel $S1P_1$ Agonist That Does Not Require S1P-Like Headgroup Interactions[S]

Pedro J. Gonzalez-Cabrera, Euijung Jo, M. Germana Sanna, Steven Brown, Nora Leaf, David Marsolais, Marie-Therese Schaeffer, Jacqueline Chapman, Michael Cameron,[1] Miguel Guerrero, Edward Roberts, and Hugh Rosen

Departments of Chemical Physiology & Immunology (P.J.G.-C., E.J., M.G.S., N.L., D.M., H.R.), Chemistry (M.G., E.R.), and the Scripps Research Institute Molecular Screening Center (M.-T.S., J.C., S.B., H.R.), La Jolla, California

Received June 19, 2008; accepted August 15, 2008

ABSTRACT

Strong evidence exists for interactions of zwitterionic phosphate and amine groups in sphingosine-1 phosphate (S1P) to conserved Arg and Glu residues present at the extracellular face of the third transmembrane domain of S1P receptors. The contribution of Arg^{120} and Glu^{121} for high-affinity ligand-receptor interactions is essential, because single-point $R^{120}A$ or $E^{121}A$ $S1P_1$ mutants neither bind S1P nor transduce S1P function. Because S1P receptors are therapeutically interesting, identifying potent selective agonists with different binding modes and in vivo efficacy is of pharmacological importance. Here we describe a modestly water-soluble highly selective $S1P_1$ agonist [2-(4-(5-(3,4-diethoxyphenyl)-1,2,4-oxadiazol-3-yl)-2,3-dihydro-1*H*-inden-1-yl amino) ethanol (CYM-5442)] that does not require Arg^{120} or Glu^{121} residues for activating $S1P_1$-dependent p42/p44 mitogen-activated protein kinase phosphorylation, which defines a new hydrophobic pocket in $S1P_1$. CYM-5442 is a full agonist in vitro for $S1P_1$ internalization, phosphorylation, and ubiquitination. It is noteworthy that CYM-5442 was a full agonist for induction and maintenance of $S1P_1$-dependent blood lymphopenia, decreasing B lymphocytes by 65% and T lymphocytes by 85% of vehicle. Induction of CYM-5442 lymphopenia was dose- and time-dependent, requiring serum concentrations in the 50 nM range. In vitro measures of $S1P_1$ activation by CYM-5442 were noncompetitively inhibited by a specific $S1P_1$ antagonist [(*R*)-3-amino-(3-hexylphenylamino)-4-oxobutylphosphonic acid (W146)], competitive for S1P, 2-amino-2-(4-octylphenethyl)propane-1,3-diol (FTY720-P), and 5-[4-phenyl-5-(trifluoromethyl)-2-thienyl]-3-[3-(trifluoromethyl)phenyl]-1,2,4-oxadiazole (SEW2871). In addition, lymphopenia induced by CYM-5442 was reversed by W146 administration or upon pharmacokinetic agonist clearance. Pharmacokinetics in mice also indicated that CYM-5442 partitions significantly in central nervous tissue. These data show that CYM-5442 activates $S1P_1$-dependent pathways in vitro and to levels of full efficacy in vivo through a hydrophobic pocket separate from the orthosteric site of S1P binding that is headgroup-dependent.

S1P is a circulating lipid that binds to five G protein-coupled receptors (GPCRs) termed $S1P_{1–5}$. $S1P_1$ selectively regulates physiological functions in the immune and cardiovascular systems, including immune cell trafficking (Rosen and Goetzl, 2005; Rosen et al., 2007) and maintaining endothelial integrity (Lee et al., 1999; Sanchez et al., 2003; Dudek et al., 2004; Sanna et al., 2006; Foss et al., 2007). Pharmacological studies with the sphingosine analog immunosuppressant prodrug FTY720 indicated that administration of FTY720 or S1P decreased lymphocyte counts in the mouse draining lymph node, resulting in lymphopenia (Mandala et al., 2002). Moreover, FTY720 was shown to be rapidly phosphorylated, with the phosphorylated species (FTY720-P)

Supported by National Institutes of Health grants AI055509, MH074404, and AI074564).

P.J.G.-C., E.J., M.G.S., and S.B. contributed equally to this work.

[1] Current affiliation: Translational Research Institute, Scripps Florida, Jupiter, Florida.

Article, publication date, and citation information can be found at http://molpharm.aspetjournals.org.
doi:10.1124/mol.108.049783.

[S] The online version of this article (available at http://molpharm.aspetjournals.org) contains supplemental material.

ABBREVIATIONS: S1P, sphingosine-1 phosphate; GPCR, G protein-coupled receptor; FTY720, 2-amino-2-(4-octylphenethyl)propane-1,3-diol; SEW2871, 5-[4-phenyl-5-(trifluoromethyl)-2-thienyl]-3-[3-(trifluoromethyl) phenyl]-1,2,4-oxadiazole; W146, (*R*)-3-amino-(3-hexylphenylamino)-4-oxobutylphosphonic acid; MS, multiple sclerosis; BBB, blood-brain barrier; TM3, transmembrane domain 3; AFD, 2-amino-4-(4-(heptyloxy)-phenyl)-2-methylbutyl dihydrogen phosphate; MAPK, mitogen-activated protein kinase; CYM-5442, 2-(4-(5-(3,4-diethoxyphenyl)-1,2,4-oxadiazol-3-yl)-2,3-dihydro-1*H*-inden-1-yl amino) ethanol; CYM-5181, 5-(3,4-diethoxyphenyl)-1,2,4-oxadiazol-3-yl; U0126, 1,4-diamino-2,3-dicyano-1,4-bis(methylthio)butadiene; CHO, Chinese hamster ovary; CRE, cAMP response element; EI, electron impact; ELISA, enzyme-linked immunosorbent assay ; LC, liquid chromatography; HPLC, high-performance liquid chromatography; FACS, fluorescence-activated cell sorting; HEK, human embryonic kidney; C.C., column chromatography.

acting as a potent agonist on $S1P_{1,\ 3-5}$ subtypes. Discovery of SEW2871 (Sanna et al., 2004), a selective agonist for $S1P_1$ that replicated the lymphopenic actions of FTY720, plus development of selective $S1P_1$ antagonists with in vivo activity, later demonstrated that $S1P_1$ was the primary mediator of lymphocyte sequestration in secondary lymphoid organs and lymphopenia.

Mechanistic insights into $S1P_1$-mediated lymphopenia came from combining genetics, pharmacological tools, and two-photon imaging (Wei et al., 2005; Sanna et al., 2006). The last of these has allowed studying real-time lymphocyte dynamics in the intact lymph node, where SEW2871 infusion reduces lymphocyte egress in the medulla, whereas a selective $S1P_1$ antagonist (W146) fully reverses agonist actions.

In the thymus, $S1P_1$ agonism enhances late thymocyte maturation yet inhibits subsequent thymocyte egress (Rosen et al., 2003; Alfonso et al., 2006; Weinreich and Hogquist, 2008). Consequently, S1P agonist administration reduces naive blood $CD4^+$ and $CD8^+$ thymocytes and B cells by nearly 90 and 70%, respectively.

Regulation of lymphocyte trafficking with $S1P_1$ agonists has opened the possibility for clinical modulation of lymphocyte dynamics, exemplified by the positive results reported in multiple sclerosis (MS) clinical trials with FTY720 (Hiestand et al., 2008). Although the mechanism of FTY720 in ameliorating MS symptoms is not clear, it may encompass multiple targets, both systemic (including $S1P_1$-mediated lymphopenia) and local, by actions on neurons (Kataoka et al., 2005; Balatoni et al., 2007; Miron et al., 2008). Vascular integrity of the blood-brain barrier (BBB) is likely to participate in the mechanism of FTY720's efficacy in MS (Foster et al., 2008). Thus, understanding the contribution of systemic and local effects of $S1P_1$ modulation would be relevant for developing efficacious therapies for autoimmune disease.

Previous studies aimed at dissecting the S1P-$S1P_1$ binding pocket have provided strong evidence for a model of S1P ligand interaction with three charged residues on $S1P_1$ (Parrill et al., 2000; Wang et al., 2001). Two residues, Arg^{120} and Glu^{121}, which are present on TM3 of all S1P receptors, interact with the phosphate headgroup and the ammonium moiety of S1P, respectively. The importance of Arg^{120} and Glu^{121} interactions with S1P has been demonstrated by mutagenesis. Substitution of Arg^{120} or Glu^{121} with alanine results in total loss of [^{33}P]S1P binding to $S1P_1$ and, consistent with the lack of binding, neither of the TM3 mutants internalizes after an S1P challenge or stimulates S1P-mediated guanosine 5′-*O*-(γ-[^{35}S]thio)triphosphate binding. Thus, the strong zwitterionic nature of S1P requires hydrophilic

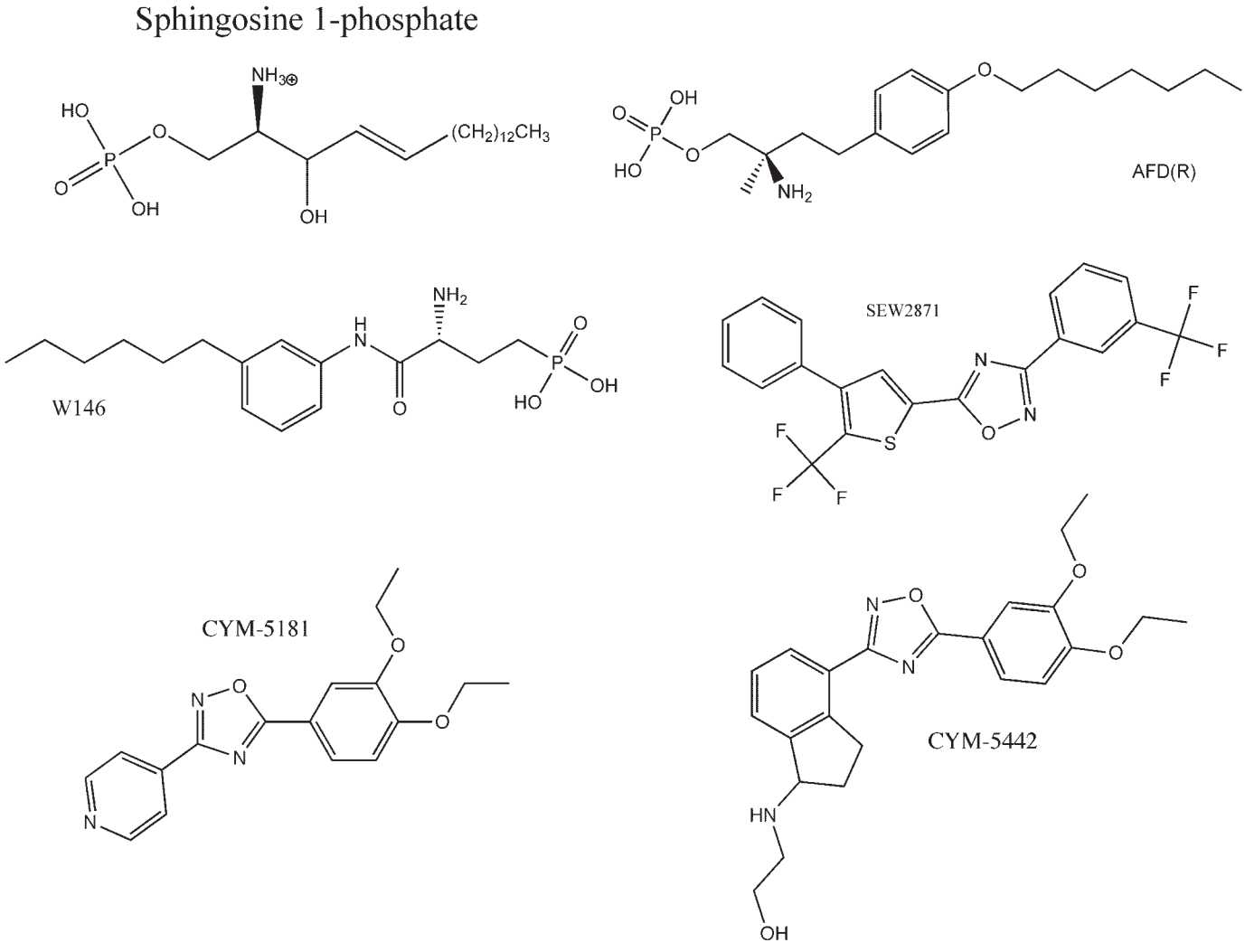

Fig. 1. Chemical structure of ligands used in this study.

headgroup interactions on $S1P_1$ TM3 Arg and Glu residues to achieve high-affinity binding and receptor functions.

We have shown that besides S1P, other $S1P_1$ agonists, including AFD-R (an FTY720-P analog) and SEW2871, also require Arg^{120} and Glu^{121} for full activation of intracellular pathways (Jo et al., 2005). It is noteworthy that although SEW2871 lacks structurally charged headgroups, its binding model to $S1P_1$ and activation of P42/p44 MAPK and AKT pathways is dependent on Arg^{120} and Glu^{121}, likely by replacing the salt-bridge polar interactions by ion-dipole interactions. SEW2871 has recently been shown to make additional hydrophobic interactions deep in $S1P_1$ TM5, suggesting that it overlaps both the hydrophilic pocket and a hydrophobic pocket on $S1P_1$ (Fujiwara et al., 2007).

Because the Arg and Glu residues are invariant across S1P receptors, developing efficacious ligands that bind solely in deep hydrophobic pockets could provide advantages for selectivity, mechanism-based toxicity, and the ability of these molecules to potentially traverse impermeant barriers, such as the BBB.

Here we report development and characterization of a potent and moderately water-soluble small molecule $S1P_1$-agonist (CYM-5442) that does not require interactions with either Arg120 or Glu121 of $S1P_1$ headgroup yet is fully active in vivo for inducing lymphopenia. It is noteworthy that CYM-5442 partitions significantly into brain tissue. Development of in vivo-active $S1P_1$ agonists that do not require headgroup interactions, such as CYM-5442, reveal a discrete novel hydrophobic pocket on $S1P_1$ to be further explored in therapeutics.

Materials and Methods

Reagents

S1P was purchased from BIOMOL Research Laboratories (Plymouth Meeting, PA). The selective $S1P_1$ agonist SEW2871 was purchased from Maybridge (Cornwall, UK). The selective $S1P_1$ antagonist W146 was from Avanti Polar Lipids (Alabaster, AL). The selective $S1P_2$ antagonist JTE-013 was from Cayman Medical Company. [^{32}P]Orthophosphate was purchased from PerkinElmer Life and Analytical Sciences. The MEK1 inhibitor U0126 was from Calbiochem (San Diego, CA).

Cell Lines

The generation of stable CHO-K1-S1P receptor cell clones and the conditions for CRE and nuclear factor of activated T cells reporter assays have been documented (Schurer et al., 2008). The Tango $S1P_4$ and Tango $S1P_5$ stable cell lines were obtained from Invitrogen and assayed according to Invitrogen's protocols with 1 μM S1P as positive control (Schurer et al., 2008). HEK293 cells stably expressing human $S1P_1$ tagged with C-terminal GFP ($S1P_1$-GFP) were a gift from Timothy Hla (University of Connecticut Health Center, Farmington, CT). $S1P_1$-GFP cells were grown as reported (Gonzalez-Cabrera et al., 2007). Parental CHO-K1 cells used in transient transfection experiments were purchased from the American Type Culture Collection (Manassas, VA).

Chemical Synthesis of CYM-5442

The schematic steps (i–iv) of CYM-5442 synthesis are indicated in Fig. 2 and are as follows.

i: 1-Hydroxy-2,3-dihydro-1*H*-indene-4-carbonitrile. To a stirred suspension of 1-oxo-2,3-dihydro-1*H*-indene-4-carbonitrile (1.0 equiv, 0.4 M) and silica gel (catalytic) in ethanol at 0°C was added $NaBH_4$ (0.33 equiv). The reaction was allowed to warm up to room temperature and stirred for 2 h. The solvent was removed under reduced pressure, and the product was purified by C.C. in hexane/EtOAc (5:5) to offer 1-hydroxy-2,3-dihydro-1*H*-indene-4-carbonitrile as white solid in 80% yield. ^{1}H NMR (300 MHz, $CDCl_3$): δ 7.62 (d, J = 7.5 Hz, 1H), 7.54 (d, J = 7.8 Hz, 1H), 7.33 (t, J = 7.8 Hz, 1H), 5.28 (t, J = 6.3 Hz, 1H), 3.28–3.18 (m, 1H), 3.02–2.92 (m, 1H), 2.63–2.52 (m, 1H), 2.06–1.99 (m, 1H).

ii: 1,*N*-Dihydroxy-indan-4-carboxamidine. To a stirred suspension of hydroxylamine hydrochloride (1.1 equiv) and Na_2CO_3 (1.1 equiv) in ethanol was added, in one portion, the benzonitrile prepared in the previous step (1 equiv). The mixture was refluxed for 6 h followed by addition of another portion of hydroxylamine hydrochloride (1.1 equiv) and Na_2CO_3 (1.1 equiv). The reaction was refluxed for an additional 6 h. The suspension was cooled to room temperature and filtered. The solid was washed with ethanol, and the filtrate was concentrated under reduced pressure. The amidoxime-crude was recrystallized from EtOAc/hexanes and used without further purification.

iii: 4-[5-(3,4-Diethoxy-phenyl)-[1,2,4]oxadiazol-3-yl]-indan-1-ol. In a microwave vial, a stirring solution of 3,4-diethoxybenzoic acid (1 equiv, 0.2M) in dimethylformamide was treated with hydroxybenzotriazole (1.3 equiv) and 1-ethyl-3-(3-dimethylaminopropyl)carbodiimide hydrochloride (1.3 equiv) at room temperature. The reaction was stirred for 20 min followed by addition, in a single portion, of amidoxime (prepared in previous step) (1.1 equiv). The reaction was stirred for additional 30 min at room temperature and then heated to 130°C for 30 min. The reaction was diluted using a saturated solution of NaCl and extracted with EtOAc (3×). The organic phase was dried over Na_2SO_4 anhydrous and concentrated under reduced pressure. The product was purified by C.C. using CH_2Cl_2:MeOH (9:1) to offer diaryloxadiazole as white solid in good yield. ^{1}H NMR (400 MHz, $CDCl_3$): δ 8.10 (d, J = 7.6, 1H), 7.78 (dd, $J1$ = 1.6 Hz, $J2$ = 8 Hz, 1H), 7.67 (d, J = 1.6 Hz, 1H), 7.56 (d, J = 7.6 Hz, 1H), 7.39 (t, J = 7.6 Hz, 1H), 6.97 (d, J = 8.0 Hz, 1H), 5.29 (t, J = 6.4 Hz, 1H), 4.19 (q, J = 7.2 Hz, 2H), 4.18 (q, J = 7.2 Hz, 2H), 3.51–4.43 (m, 1H), 3.22–3.14 (m, 1H), 2.59–2.51 (m, 1H), 2.04–1.97 (m, 1H), 1.5 (t, J = 7.2 Hz, 3H), 1.49 (t, J = 7.2, 3H); ^{13}C NMR (100 MHz, $CDCl_3$): δ 175.2, 168.9, 152.8, 148.9, 146.6, 143.3, 128.9, 127.4,

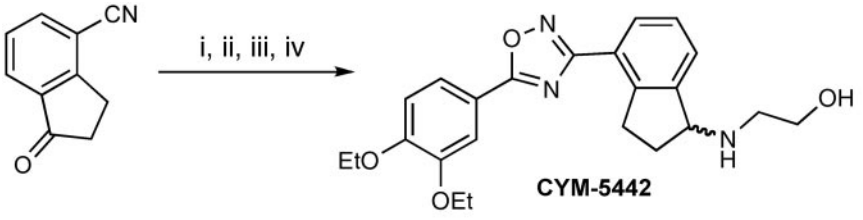

i.- $NaBH_4$, SiO_2, EtOH, 0 °C to r.t., 2h. ii.- $NH_2OH.HCl$, Na_2CO_3, EtOH, reflux, 12h. iii.- 3,4-diethoxybenzoic acid, EDCI, HOBt, DMF, 130 °C, m.w., 30min. iv.- (a) $SOCl_2$, Py, r.t., 2h. (b) Aminoethanol, DIPEA, DMF, 50 °C, 48h.

Fig. 2. Chemical synthesis of CYM-5442.

127.0, 123.8, 122.2, 116.7, 112.7, 112.4, 76.2, 64.9, 64.8, 35.7, 31.5, 14.9, 14.8. Mass spectrometry (EI) m/z 367 (M^+), high-resolution mass spectrometry (EI) for $C_{21}H_{22}N_2O_4$ (M^+): calculated, 367.1652; found, 367.1653.

iv: 2-{4-[5-(3,4-Diethoxy-phenyl)-[1,2,4]oxadiazol-3-yl]-indan-1-ylamino}-ethanol. A solution of alcohol (1 equiv), at 0°C, was treated with $SOCl_2$ (1.1 equiv) and pyridine (1.1 equiv) in CH_2Cl_2. The reaction was stirred at room temperature for 2h. The reaction was diluted with CH_2Cl_2 and washed with $NaHCO_3$ (2×). The organic phase was dried over sodium sulfate and concentrated under reduced pressure. The crude was dissolved in dimethylformamide and treated with the ethanolamine (2 equiv) and diisopropylethylamine (2.0 equiv). The reaction was stirred at 50°C for 48 h. The reaction was diluted with H_2O and the product extracted with EtOAc (3×). The product was purified by C.C. using CH_2Cl_2/MeOH (9:1) to offer aminoethanol CYM-5442 as white solid in 60% yield. ^{1}H NMR (500 MHz, $CDCl_3$): δ 8.12 (d, J = 7.5 Hz, 1H), 7.79 (dd, $J1$ = 2.0 Hz $J2$ = 8.5 Hz, 1H), 7.68 (d, J = 2.0 Hz, 1H), 7.63 (d, J = 7.5 Hz, 1H), 7.40–7.37 (m, 1H), 4.49–4.47 (m, 1H), 4.23–4.16 (m, 4H), 3.78–3.70 (m, 1H), 3.53–3.46 (m, 1H), 3.29–3.22 (m, 1H), 2.96–2.94 (m, 4H), 2.56–2.50 (m, 1H), 2.09–2.03 (m, 1H), 1.52–1.49 (m, 6H); ^{13}C NMR (125 MHz, $CDCl_3$): δ 175.03, 168.66, 152.71, 148.87, 143.76, 128.71, 127.11, 123.89, 122.04, 116.67, 112.63, 112.49, 104.66, 64.84, 64.61, 62.70, 60.34, 47.98, 31.90, 29.69, 14.72, 14.64. Mass spectrometry (EI) m/z 410 (M^+), high-resolution mass spectrometry (EI) for $C_{23}H_{27}N_3O_4$ (M^+): calculated, 410.2074; found, 410.2077.

Evaluation of CYM-5442 Agonist Properties

Details of the screening CRE reporter assays can be found in Schurer et al., (2008). For the CRE reporter assay studies, forskolin was included at a 2 μM final concentration before addition of the agonists. Agonist-mediated inhibition of forskolin induced cAMP accumulation was read on an Envision fluorescent plate reader (384-well format) after 2-h agonist incubation and with SEW2871 as the positive control. Agonist-induced S1P$_1$-GFP internalization and ubiquitination assays have been documented previously (Gonzalez-Cabrera et al., 2007). Description of agonist-mediated S1P$_1$-GFP phosphorylation experiments can be found in Schurer et al., (2008).

ELISA Determination of p42/p44 MAPK Activity

CYM-5442 and S1P-mediated p42/p44 MAPK activation was measured using an ELISA kit (Cell Signaling Technologies, Danvers, MA) in CHO-K1 cells transiently transfected with either the WT S1P$_1$ receptor cDNA or the single-point S1P$_1$ mutant (R^{120}A or E^{121}A) cDNAs (gifts from Gabor J. Tigyi, University of Tennessee Health Science Center, Memphis, TN). For transfections, cells were plated on 10-cm dishes at 80% confluence and transfected with 12 μg of each plasmid using Fugene HD (Roche Applied Science, Indianapolis, IN) in Opti-MEM (Invitrogen). After 16 h, each pool-transfected dish was split into a six-well plate and allowed to incubate for additional 24 h. The cells were next incubated for 4 h in serum-free Dulbecco's modified Eagle's medium before addition of the agonist. In the antagonist (W146)/MEK1 inhibitor (U0126) experiments, W146 or U0126 was incubated for 30 min (U0126) or 1 h (W146), respectively, at 10 μM before agonist treatment. Cells were then stimulated for 5 min (determined empirically to be maximal for both agonists) with increasing concentrations of CYM-5442 or S1P and activation of p42/p44 MAPK phosphorylation was assayed according to manufacturer instructions. For each condition (WT, R^{120}A, or E^{121}A), both CYM-5442 and S1P agonists were tested in parallel, in the presence and absence of W146. In addition, for each of the conditions tested, the concentration response curves for agonist-mediated activation of p42/p44 MAPK phosphorylation were plotted as a percentage of the agonist eliciting the maximal response, and the potency (EC_{50}), maximal response (E_{max}), and goodness of fit (R^2) values were determined using Prism (Graphpad Software, San Diego, CA).

TABLE 1

Selectivity of CYM-5442 for the cloned human S1P receptors

In agonist format, CYM-5442 was tested in 12-point (up to 10 μM) concentration response curves. In antagonist format, CYM-5442 was included in the assay at 10 μM final concentration and tested for its potential to block an EC_{80} concentration of S1P.

Receptor Subtype	Agonist Format (E_{max}/EC_{50})	Antagonist Format (IC_{50})
S1P$_1$[a]	100%/1.35 ± 0.25 nM	N.A.
S1P$_2$[b]	N.A.	N.A.
S1P$_3$[c]	N.A.	N.A
S1P$_4$[d]	N.A.	N.D.
S1P$_5$[e]	20% at 10 μM	N.D.

N.A., no activity; N.D., not determined

[a] Agonist format measured forskolin-stimulated CYM-5442 inhibiton of cAMP CRE transcription on stable S1P$_1$-CHO-K1-CRE-bla cells, with SEW2871 as positive control. W146 inhibition of SEW2871 was used as a positive control in the antagonist format.

[b] Agonist format measured CYM-5442-stimulated cAMP accumulation on stable CHO-K1-S1P$_2$-CRE cells with S1P as positive control. JTE-013 (Cayman Chemical, Ann Arbor, MI) inhibition of S1P was used as positive control in antagonist format.

[c] Agonist format measured CYM-5442-stimulated cAMP accumulation in stable S1P$_3$-nuclear factor of activated T cells-bla-CHO-K1 cells with S1P as positive control.

[d] Agonist format measured CYM-5442-stimulated β-arrestin activation in stable Tango S1P$_4$-bla U2OS cells with S1P as positive control.

[e] Agonist format measured CYM-5442-stimulated cAMP accumulation in stable Tango S1P$_5$-bla U2OS cells with S1P as positive control.

Pharmacokinetic Studies

Pharmacokinetics of CYM-5442 was assessed in Sprague-Dawley rats. The compound was formulated at 1 mg/ml [10:10:80 dimethyl sulfoxide/Tween 80/water (v/v/v)] and dosed at 1 mg/kg intravenous (i.v.) into the jugular or 2 mg/kg by oral gavage (p.o.). Blood was obtained at t = 5, 15, or 30 min or 1, 2, 4, 6, and 8 h into EDTA-containing tubes, and plasma was generated by standard centrifugation methods. Separate studies to evaluate brain exposure were done in C57BL6 mice in which CYM-5442 was dosed at 10 mg/kg by intraperitoneal (i.p.) route. Blood and brains were obtained at t = 2 h to assess the amount of compound in the target organ. All procedures and handling were according to standard operating procedures approved by the Institutional Animal Care and Use Committee (IACUC).

To assess in vivo pharmacokinetic parameters an LC-tandem mass spectrometry bioanalytical method was developed in which 25 μl of plasma was treated with 125 μl of acetonitrile containing an internal standard in a Multiscreen Solvinter 0.45-μm low binding polytetrafluoroethylene hydrophilic filter plate (Millipore, Billerica, MA) and allowed to shake at room temperature for 5 min. The plate was then centrifuged for 5 min at 4000 rpm in a tabletop centrifuge, and the filtrate was collected in a polypropylene capture plate. The filtrate (10 μl) was injected using an HPLC (1200; Agilent Technol-

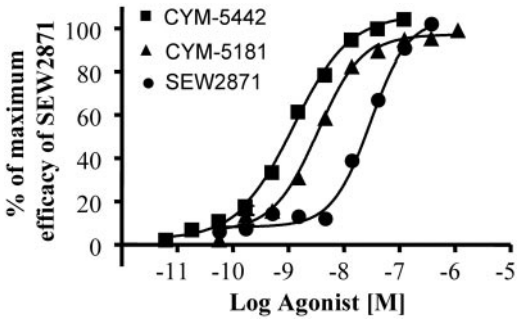

Fig. 3. Concentration dependent inhibition of CRE transcription in stable S1P$_1$-CHO cells by S1P$_1$ agonists. Cells stably expressing a CRE-β-lactamase reporter and human S1P$_1$ were incubated with increasing concentrations of SEW2871, CYM-5442, or CYM5181. The ability of the agonists to inhibit forskolin-stimulated β-lactamase expression was measured as described previously (Schurer et al., 2008). The potency (pEC_{50}) values were determined to be −7.54, −8.47, and −8.91 for SEW2871, CYM5181, and CYM-5442, respectively.

ogies, Santa Clara, CA) equipped with a Betasil C18 HPLC column 5 μ (50 × 2.1 mm; Thermo Fisher Scientific, Waltham, MA). Mobile phase A was water with 0.1% formic acid. Mobile phase B was acetonitrile with 0.1% formic acid. Flow rate was 375 μl/min using a gradient of 90% A/10% B from 0 to 0.5 min, ramped to 5% A/95% B at 2 min, held at 5% A/95% B until 3.0 min, ramped to 90% A/10% B at 4 min, and held at 90% A/10% B until 7 min. An LC-tandem mass spectrometry system (API 4000; Applied Biosystems/MDS Sciex (Foster City, CA), equipped with a turbo ion spray source, was used for all analytical measurements. Instrument settings had curtain gas set to 10, gas 1 and gas 2 set to 45, ionization energy set to 5500 V, drying gas temperature 550°C, resolution was set to unit, and dwell time was set to 100 ms. A positive ion MRM method was developed. CYM-5442 was quantitated from 2 to 1000 ng/ml. Peak areas of the *m/z* 410.1→193.1 product ion of CYM-5442 (dicluster potential = 45, collision energy = 30) were measured against the peak areas of the internal standard (sunitinib) *m/z* 399→283 product ion (DP = 86, CE = 41). Data were fit using WinNonLin (Pharsight Corporation, Mountain View, CA).

Similar conditions were used to determine brain levels of CYM-5442 except that the brain samples were frozen upon collection. When analyzed, the frozen samples were weighed and acetonitrile was added [10× (w/v)]. The samples were sonicated to extract the compound from the brain matrix and then filtered as described above. Brain samples were analyzed against a standard curve generated in blank brain matrix.

Measurement of CYM-5442-Mediated Lymphopenia

Male C57BL6 mice weighing 30 g were used for all experiments. All animal studies were approved by the IACUC. Animals were injected intraperitoneally with a volume of 300 μl with the indicated dose of CYM-5442 or vehicle. For W146 experiments, mice were administered with 20 mg/kg W146 or vehicle for 30 min before CYM-5442 administration. Vehicle consisted of sterile water (CYM-5442) or 10% dimethyl sulfoxide and 25% Tween 20 in sterile water (W146). After incubation at the indicated times, animals were euthanized, and blood was collected into tubes containing EDTA. White

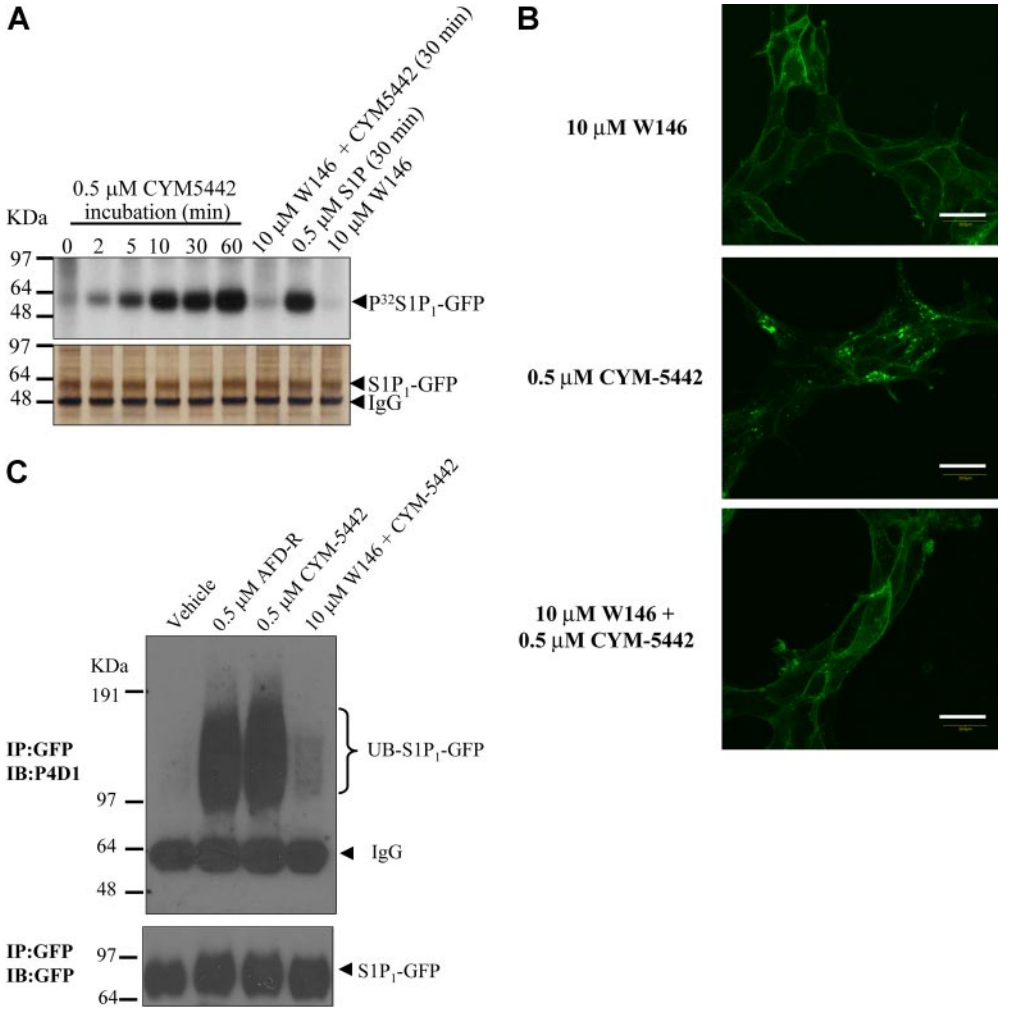

Fig. 4. CYM-5442 activates three $S1P_1$-dependent pathways in stable $S1P_1$-GFP 293 cells. The ability of CYM-5442 to stimulate $S1P_1$ phosphorylation, $S1P_1$ internalization, and $S1P_1$ ubiquitylation was measured in HEK293 cells expressing human $S1P_1$ tagged to C-terminal GFP. A, time-dependent induction of $S1P_1$ phosphorylation by CYM-5442 is abolished by the $S1P_1$ antagonist W146. Orthophosphate-P^{32} labeled cells were incubated with CYM-5442 for the indicated times, followed by $S1P_1$ immunoprecipitation using GFP. Immunoprecipitates were then run by SDS-polyacrylamide gel electrophoresis and exposed to determine whole receptor phosphorylation status. The silver-stained gel (bottom) confirmed equal loading of immunoprecipitated $S1P_1$-GFP across conditions. The mass ladder is indicated in kilodaltons. B, CYM-5442 stimulates internalization of $S1P_1$-GFP from the plasma membrane into cytoplasmic vesicles (at 45-min incubation, middle), whereas W146 preincubation (30 min, bottom) blocks CYM-5442-mediated internalization. W146 alone had no effect on internalization (top). Representative micrographs are shown (n = 3); 20-μm scale bar; 40×. C, CYM-5442 induces $S1P_1$ ubiquitylation (UB-$S1P_1$-GFP) by similar magnitude versus the full, nonselective S1P receptor agonist, AFD-R (top immunoblot). Note that CYM-5442 ubiquitylation is abolished by W146 preincubation. For this experiment, AFD-R and CYM-5442 were incubated for 1 h and W146 was included 30 min before CYM-5442 stimulation. Equal loading of immunoprecipitated $S1P_1$ receptor was confirmed by reblotting for GFP (bottom immunoblot). The mass ladder is indicated in kilodaltons. This experiment was repeated twice with similar results.

blood cell count and lymphocyte counts were obtained using an automated veterinary Hemoanalyzer (Hospitex Diagnostics, Webster, TX) by reading 30-μl blood samples. The remaining blood was used for determination of drug serum levels (see below), or to determine, by FACS, the number of B cells (using a fluorescein isothiocyanate-conjugated B220 antibody marker; 1:100 dilution; BD Diagnostics, Franklin Lakes, NJ) and T cells (using Pacific Blue CD4$^+$ and Per-CP-Cy5.5 CD8$^+$ antibodies; both at 1:100; BD Diagnostics). FACS analysis was done in FlowJo (Tree Star, Ashland, OR).

CYM-5442 and W146 Serum Concentration. Blood samples used in lymphopenia studies were further processed for measuring serum CYM-5442 and W146 concentrations. Samples (100 μl of plasma) were extracted with 400 μl of ice-cold methanol (stored at −20°C), vortexed for 1 min, allowed to sit at 4°C for 30 min, and centrifuged at 16,400 rpm for 5 min. The supernatant was evaporated to a volume near dryness, and methanol was added to bring the final volume to 50 μl. For calibration standards, clean plasma was spiked with increasing concentrations of CYM-5442 or W146 and processed the same way as the samples. Samples were analyzed on an Agilent LC-tandem mass spectrometry system using an 1100 LC stack-mated with a 6410 triple quadrupole mass spectrometer. For CYM-5442 quantification, the transition of *m/z* 410 -> 349.2 was monitored, and for W146, the transition of *m/z* 343→138 was monitored. The column used was an Agilent Zorbax SB-C18 (2.1 × 75 mm). Flow rate was 250 μl/min. Mobile phase A = water/0.1% formic acid; mobile phase B = acetonitrile/0.1% formic acid. Gradient: 15% B at T = 0 ramped to 98% B at T = 8; 5 μl injected.

Results

CYM-5442 Is a Potent S1P$_1$-Selective Agonist. CYM-5442 (Fig. 1) is a chemically optimized version of an original hit (CYM-5181) from a screen aimed to discover novel S1P receptor agonists (Schurer at al., 2008). The chemical synthesis of CYM-5442 is depicted in Fig. 2. Even though CYM-5442 contains the privileged oxadiazole-based scaffold reported to fit S1P receptors (Schurer et al., 2008), CYM-5442 is selective for S1P$_1$, as measured by high-throughout agonist-antagonist formats across S1P receptors (Table 1). In high-throughput agonist format with SEW2871 as the positive control, CYM-5442 inhibited forskolin-stimulated CRE transcription in a concentration-dependent manner (Fig. 3), being a full agonist compared with SEW2871 but of higher potency (20- and 100-fold) relative to CYM-5181 and SEW2871, respectively.

Further characterization of the agonist properties of CYM-5442 was done using a receptor immunoprecipitation protocol previously validated for studying trafficking and fate of S1P$_1$-GFP during agonist stimulation (Gonzalez-Cabrera et al., 2007). Using this protocol and HEK293 cells stably expressing S1P$_1$ fused to GFP on the carboxyl terminus, we probed CYM-5442 for stimulating three agonist-S1P$_1$ activated steps: receptor phosphorylation, receptor internalization and receptor-ubiquitin recruitment. Figure 4A indicates that incubation of 500 nM CYM-5442 with [^{32}P]orthophosphate-labeled cells stimulated S1P$_1$ phosphorylation in a time-dependent manner, similar to that obtained with 500 nM S1P (at 30 min). CYM-5442 led to rapid S1P$_1$ phosphorylation that was sustained throughout the analysis. To confirm the involvement of S1P$_1$ for CYM-5442 phosphorylation, the S1P$_1$ selective antagonist W146 was used. Preincubation with 10 μM of W146 for 30 min before CYM-5442 treatment completely abolished CYM-5442-mediated S1P$_1$ phosphorylation, whereas antagonist alone had no effect on the response. In addition, silver staining of the same gel used to measure receptor phosphorylation indicated that the differences in S1P$_1$ phosphorylation across conditions were not due to differences in immunoprecipitated S1P$_1$ protein loading.

Membrane-associated GPCRs are usually internalized into cytosolic vesicles upon agonist stimulation. We and others have shown that S1P and S1P agonist analogs internalize S1P$_1$-GFP from the plasma membrane to cytoplasmic vesicles (Liu et al., 1999; Gonzalez-Cabrera et al., 2007; Oo et al., 2007). Figure 4B shows that incubation of S1P$_1$-GFP cells with 500 nM CYM-5442 stimulated the internalization of S1P$_1$-GFP receptor from a membrane-associated localization to an intracellular, multivesicular compartment. Similar internalization pattern was obtained by 0.5 μM S1P incubation (not shown). Internalization of S1P$_1$-GFP by CYM-5442 was completely blocked by preincubation with 10 μM W146, and, consistent with the phosphorylation data, W146 alone had no effect on internalization.

S1P$_1$ agonism with some ligands, termed supraphysiological because of their ability to alter receptor signaling reserve, results in degradation of S1P$_1$-GFP in lysosomes and proteasomes, and the magnitude of agonist-dependent receptor ubiquitination has been reported to influence receptor fate

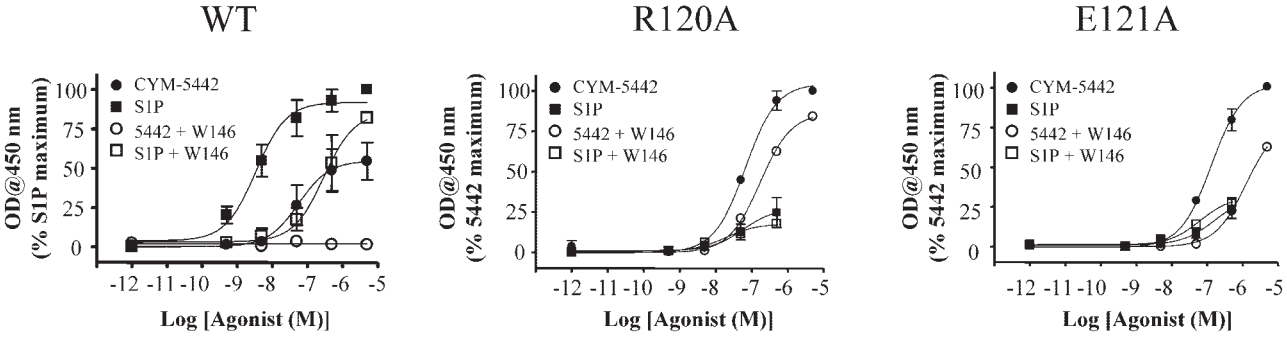

Fig. 5. CYM-5442 does not require two essential S1P headgroup receptor interactions for activating p42/p44 MAPK. Wild-type (WT) human S1P$_1$ and two single-point S1P$_1$ receptor mutants (R^{120}A and E^{121}A), reported to independently disrupt S1P-S1P$_1$ binding and/or S1P-S1P$_1$ function, were transiently transfected into CHO-K1 cells. After 48 h, cells were stimulated for 5 min with increasing concentrations of S1P or CYM-5442, and agonist-dependent S1P$_1$ activation of p42/p44 MAPK activity was determined using ELISA studies. Parallel agonist concentration responses were also performed with cells that had been preincubated with 10 μM W146 for 30 min. For each of the three conditions, the fitted curves are the mean ± S.D. of three independent experiments. The potency (pEC$_{50}$), intrinsic activity (E_{max}) and goodness of fit (R^2) derived from the agonists' activation curves were determined for WT, R^{120}A, and E^{121}A transfected cells, both in the absence (−) or presence (+) of the S1P$_1$ antagonist W146. These values are shown in Table 1.

(Gonzalez-Cabrera et al., 2007; Oo et al., 2007). Thus, agonist recruitment of ubiquitin to $S1P_1$ can be used as a measure of ligand receptor activation. The ability of AFD-R, a highly efficient ubiquitinator (Gonzalez-Cabrera et al., 2007; Oo et al., 2007), and CYM-5442 to recruit ubiquitin onto immunoprecipitated $S1P_1$-GFP is shown in Fig. 4C. CYM-5442 stimulated receptor ubiquitination (UB-$S1P_1$-GFP) to AFD-R levels. Ubiquitination by the agonists resulted in high molecular mass smears (approximately from 97 to 180 kDa) of ubiquitin-receptor complexes running immediately above the immunoprecipitated receptor. Preincubation with the selective antagonist W146 was shown to nearly abolish CYM-5442-stimulated $S1P_1$ ubiquitination. Overall, the in vitro data indicate that CYM-5442 is a potent and selective $S1P_1$ agonist.

CYM-5442 Does Not Require Ionic S1P-receptor Headgroup Interactions for Activating $S1P_1$-Mediated p42/p44 MAPK Phosphorylation. S1P and synthetic $S1P_1$ agonists have been shown to activate the mitogenic p42/p44-MAPK pathway across many cell types (Sorensen et al., 2003; Jo et al., 2005; Ahmad et al., 2006). The ability of CYM-5442 and S1P to activate p42/p44-MAPK was studied by ELISA, using lysates of CHO-K1 cells transiently expressing either the human wild-type $S1P_1$ (WT) or the two separate single-point $S1P_1$ mutants (R^{120}A and E^{121}A), known to abolish binding and activity of S1P on $S1P_1$. Time course studies demonstrated that maximal p42/p44-MAPK activity was achieved at 5 min in CHO-K1 cells expressing $S1P_1$ (Supplemental Fig. 1A). The time course also showed that treatment with 500 nM S1P for 5 min did not lead to measurable p42/p44 MAPK activity in mock-transfected CHO-K1 cells. S1P and CYM-5442 stimulated P42/P44 MAPK phosphorylation was completely blocked by preincubation with 10 μM U0126, a MEK1 inhibitor (Supplemental Fig. 1B).

Using the 5-min incubation time, we sought to determine the requirement of $S1P_1$ Arg^{120} and Glu^{121} residues for CYM-5442 and/or S1P activation of P42/P44 MAPK. For these experiments, concentration response curves with the agonists were performed on cells expressing each of the single-point mutants (R^{120}A and E^{121}A), and these responses were compared with those in the WT receptor, in both the presence and the absence of the selective $S1P_1$ antagonist W146. Figure 5 shows the plots of the average concentration responses in the three transfectants, whereas the potency (EC_{50}), maximal response (E_{max}), and goodness of fit (R^2) value estimates derived from curve fitting are included in Table 2. In WT cells, both S1P and CYM-5442 led to the concentration-dependent activation of P42/P44 MAPK phosphorylation, with EC_{50} values of 2.3 and 46 nM, respectively. In WT transiently transfected CHO-K1 cells, S1P was a full agonist (E_{max} of 1.0 or 100%), whereas CYM-5442 was a partial agonist (E_{max} of 0.7 or 70% of S1P). Incubation of 10 μM W146 before addition of S1P resulted in a significant rightward shift (60-fold, EC_{50} of 140 nM) in potency of S1P versus S1P alone (Fig. 5). On the other hand, preincubation with W146 in WT cells led to the complete inhibition of CYM-5442-mediated p42/p44 MAPK phosphorylation (Fig. 5). These results indicate that W146 is a competitive antagonist with S1P and a noncompetitive antagonist against CYM-5442.

As expected, substitution of $S1P_1$ Arg^{120} for alanine (R^{120}A) resulted in a near loss of p42/p44 MAPK activity for S1P. Curve-fitting the S1P data in this mutant indicated relatively poor fits ($R^2 < 0.4$). It is noteworthy that the R^{120}A mutant was still able to maintain p42/p44 MAPK activity when incubated with CYM-5442; as a result, the data were plotted relative to CYM-5442 maximum. The EC_{50} for CYM-5442 in the R^{120}A mutant was determined to be not significantly different from that of WT CYM-5442 cells (R^{120}A EC_{50}, 67 nM; WT EC_{50}, 46 nM). Unlike WT cells, preincubation of 10 μM W146 in mutant R^{120}A cells did not significantly alter the p42/p44 MAPK activity by CYM-5442, and led to a modest (3-fold) rightward shift in EC_{50} (67 nM), suggesting that in the absence of headgroup localization, W146 is a weak competitive antagonist of the hydrophobic site.

Consistent with the notion that S1P makes a functional headgroup interaction with Glu^{121}, S1P did not lead to significant p42/p44 MAPK activation in E^{121}A $S1P_1$ mutant cells. On the other hand, activation of p42/p44 MAPK by CYM-5442 in E^{121}A $S1P_1$ cells was concentration dependent, with a mean EC_{50} value of 134 nM. W146 preincubation led to a 10-fold rightward shift in potency of CYM-5442 for activating p42/p44 MAPK phosphorylation in E^{121}A transfected cells. These results indicate that for $S1P_1$-dependent p42/p44 MAPK activation, CYM-5442 does not require the Arg^{120} and Glu^{121} $S1P_1$ residues that make up functional S1P-$S1P_1$ headgroup interactions.

CYM-5442 Pharmacokinetics. We next evaluated the pharmacokinetics of CYM-5442 in rats. Measures included are depicted in Table 3. Overall, CYM-5442 was modestly orally bioavailable (F = 26%). Routes of delivery influenced the half-lives ($t_{1/2}$) of 50 min (intravenous) and 3 h (oral), which supported its use in vivo. It is noteworthy that in mice, CYM-5442 administration was highly central nervous system-penetrant. A dose of 10 mg/kg i.p. for 2 h resulted in a 13.7 ± 2.9 μM concentrations in brain compared with 1.08 ± 0.3 μM in plasma. This brain-to-plasma ratio of approximately 13:1 suggests that CYM-5442 may be a useful tool for studying the roles of $S1P_1$ in the central nervous system.

TABLE 2

CYM-5442 does not require essential S1P headgroup-receptor interactions for activating p42/p44 MAPK

Mean potency (EC_{50}), intrinsic activity (E_{max}), and goodness of fit (R^2) values for the S1P and CYM-5442 response curves depicted in Figure 4. Minus (−) and plus (+) refer to the presence or absence of 10 μM W146 in the assay.

	WT				R^{120}A				E^{121}A			
	S1P		5442		S1P		5442		S1P		5442	
	−	+	−	+	−	+	−	+	−	+	−	+
$LogEC_{50}$	−8.6	−6.8	−7.3	−5.7	−7.2	−7.7	−7.2	−6.8	−6.8	−7.2	−6.9	−5.9
E_{max} (%)	100	90	70	7	25	17	100	86	27	27	100	80
R^2	0.98	0.98	0.95	N.F.	N.F.	N.F.	0.98	0.99	N.F.	N.F.	0.99	0.79

N.F., no fit

CYM-5442 Induces and Maintains Lymphopenia in Mice through S1P$_1$ Activation. Administration of S1P$_1$ agonists such as SEW2871 or FTY720-P induces rapid and reversible lymphopenia in mice (Mandala et al., 2002; Sanna et al., 2004). To determine whether CYM-5442 could lead to the induction of lymphopenia, we treated mice with a dose of 10 mg/kg i.p. and compared whole-blood white blood cell count and the number of circulating B and T cells against vehicle-treated mice. A 5-h treatment protocol was chosen based on the pharmacokinetic data (Table 3). White blood cell counts in CYM-5442 animals were decreased by 64% versus vehicle at 5 h (Table 4). FACS analyses of whole blood from treated animals indicated that CYM-5442 decreased B220$^+$ B cells by 63% compared with vehicle, whereas CD4$^+$ and CD8$^+$ T-cell counts were decreased by 83% and 84% of vehicle, respectively. These data indicate that a single dose of CYM-5442 induces acute lymphopenia in mice.

To ascertain whether the effects of CYM-5442 were dose-dependent, we employed a 5-h treatment and a dosing range of 0.3 to 10 mg/kg. The dose-response of CYM-5442 for inhibiting CD4$^+$ and CD8$^+$ cell populations is shown in Fig. 6A, and a representative example of the FACS scatter plots in individual mice is shown in Fig. 6B. The data indicates that CYM-5442 decreased CD4$^+$ and CD8$^+$ cell counts in a dose-dependent manner, attaining near-maximal effects on inhibition of these cell populations at serum CYM-5442 levels that ranged between 50 and 100 nM. Overall, the CYM-5442 mediated inhibition of B cell and T cell number had an estimated ED$_{50}$ of 0.5, 2.0, and 1.0 mg/kg for CD4$^+$, CD8$^+$, and B220$^+$, respectively (Fig. 6C).

Next, we measured the time course for CYM-5442 mediated lymphopenia and whether CYM-5442 effects could be reversed upon agonist clearance from plasma. These studies were performed employing a 16-h window, and both B- and T-cell counts were determined in conjunction with measures of serum CYM-5442 drug levels from the same animals (Fig. 6D). A representative example of individual animal FACS scatter plots is shown in Fig. 6E. With a fixed dose of 10 mg/kg, shown in Fig. 5A to be maximal for CYM-5442 induction of B-cell and T-cell lymphopenia, the data indicates that CYM-5442 CD4$^+$ and CD8$^+$ counts dropped significantly during the first 3 h of administration, and seemed to be maintained at these low levels from 3 h to 5 h. After 5 h, the B- and T-cell counts began to reverse toward basal levels; consistent with the time in which CYM-5442 began to disappear from plasma. Consistent with the dose-response data on Fig. 5A, CYM-5442 induction and maintenance of lymphopenia in the time course study occurred at serum levels of CYM-5442 ranging between 50 and 100 nM. The direct relationship between B- and T-cell recovery and loss of plasma serum CYM-5442 content thus suggested that CYM-5442-mediated lymphopenia can be reversed upon CYM-5442 clearance from the organism.

The minimal signal for lymphocyte sequestration and induction of lymphopenia by S1P$_1$ agonists depends on activation of S1P$_1$. To ascertain whether the in vivo effects of CYM-5442 were due to S1P$_1$ receptor activation, we used the selective S1P$_1$ antagonist, W146, shown here to block all of the measures of CYM-5442 activation in vitro. For antagonist studies, we used a 5-h window and a dose of CYM-5442 of 2 mg/kg, which is close to the ED$_{50}$ for CYM-5442 induction of B- and T-cell lymphopenia (Fig. 6, A and C). A competing dose of W146 of 20 mg/kg was first administered to mice and allowed to equilibrate for 30 min before CYM-5442 administration. Table 5 shows that at near ED$_{50}$, CYM-5442 led to the reduction of CD4$^+$, CD8$^+$, and B220$^+$ cell counts by approximately 50% of vehicle, whereas W146 was able to partially recover CYM-5442 effects on B-220$^+$, CD4$^+$, and CD8$^+$ cell counts. It is noteworthy that neither administration of W146 alone nor of vehicle had measurable effects on cell counts (data not shown). This indicates that CYM-5442-mediated lymphopenia is dependent on S1P$_1$ receptor activation.

Discussion

Using a chemical approach, we have characterized a small molecule compound, CYM-5442, as a selective and efficacious S1P$_1$ agonist for inducing and maintaining lymphopenia in vivo. It is of interest that the pharmacological properties of CYM-5442 for activating S1P$_1$-dependent pathways are distinct from S1P, in that the ligand has no groups capable of mimicking the headgroups of S1P. The data strongly suggest that CYM-5442 interacts with S1P$_1$ in a binding pocket separate from key S1P$_1$ residues Arg^{120} and Glu^{121} essential for high-affinity S1P binding and receptor activation (Parrill et al., 2000; Wang et al., 2001; Jo et al., 2005). Alternative residues of the putative hydrophobic pocket interacting with oxadiazole series of compounds, such as the original S1P$_1$ agonist screening hit CYM-5181, have been recently published by Schurer et al., (2008). Because CYM-5442 has an EC$_{50}$ within a factor of 3 of CYM-5181, the binding free energies are within experimental error of each other, and thus the docking of the ligand CYM-5442 into the receptor

TABLE 3
Pharmacokinetic parameters of CYM-5442 in rats
Formulation: 10%/10%/80% (dimethyl sulfoxide/Tween-20/water) (v/v)

Parameters	CYM-5442	
	2 mg/kg p.o.	1 mg/kg i.v.
$t_{1/2}$	4.00 ± 1.45	3.05 ± 0.37
MRT (h)	6.35 ± 2.10	3.54 ± 0.38
Cl (ml/min/kg)	360.1 ± 73.3	72.90 ± 11.70
Vss (L)	N.D.	15.60 ± 3.50
AUC (μM/h)	0.23 ± 0.053	0.57 ± 0.10
AUC (% extrap,ob)	27.80 ± 14.20	11.35 ± 14.20
C_{max} (nM)	36 ± 7.2	220.0 ± 18.0
T_{max}	1.17 ± 0.76	0.083 ± 0.00
F%	20.50 ± 4.67	N.D.

MRT, maximum retention time; Cl, clearance; Vss, volume of distribution at steady state; N.D., not determined; AUC, area under the curve; C_{max}, maximal concentration; T_{max}, maximal time; F%, oral viability.

TABLE 4
Short-term CYM-5442 administration induces lymphopenia in mice
Mice (three per group) were injected with a dose of 10 mg/kg i.p. in a 300-μl volume. Vehicle control mice received sterile water injections. Five hours after treatment, animals were euthanized and blood was collected into tubes containing EDTA. Blood lymphopenia was assessed by comparing absolute white blood cell (WBC) number between CYM-5442-treated and vehicle-treated animals, as measured with an automated hemoanalyzer. In addition, FACS analyses were used to measure blood B220-positive cells (B220$^+$, a marker for B cells), and from the B220$^-$ population, the percentage of single-positive CD4 (CD4$^+$) and CD8 (CD8$^+$) T cells.

Parameters	Vehicle	CYM-5442
WBC ($\times 10^3$/mm^3)	11.9 ± 0.2	4.3 ± 0.4*
B220$^+$ (%)	40.5 ± 0.6	14.7 ± 0.5*
CD4$^+$ (%)	11.5 ± 0.2	1.9 ± 0.2*
CD8$^+$ (%)	11.9 ± 0.3	1.9 ± 0.4*

* $P < 0.05$ vs. vehicle-treated.

pocket is the same as the model shown for CYM-5181 (Fig. 6; Schurer et al., 2008) and distinct from the head-group constrained interactions of S1P (Supplemental Fig. 5; Schurer et al., 2008). These differences between S1P and CYM-5442 find expression quantitatively by the retention of CYM-5442 activation of the $E^{121}A$ and $R^{120}A$ receptor mutants that fail to respond to S1P, as well as by the different mode of inhibition for CYM-5442 compared with S1P using the $S1P_1$ antagonist W146. Mutagenesis of either Arg^{120} or Glu^{121} residues, present on the extracellular face of TM3, to alanine has been shown to abolish S1P-$S1P_1$ binding and subsequent receptor activation (Parrill et al., 2000; Wang et al., 2001; Jo et al., 2005), due to the inability of the charged phosphate and ammonium headgroups in S1P to make polar interactions with neutral alanine on the $R^{120}A$ and $E^{121}A$ mutants. Whereas S1P stimulated MEK1-dependent p42/p44 MAPK phosphorylation in WT cells in a concentration-dependent manner, and with a potency consistent with literature values (Mandala et al., 2002; Sanna et al., 2004), neither of the mutant receptors was able to elicit significant signal when treated with S1P. On the other hand, the same single-point mutants shown to be unresponsive to S1P, were still able to fully activate MEK1-dependent p42/p44 MAPK activity when treated with CYM-5442, with potency values found to be not significantly different between WT and $R^{120}A$ receptors, although the $E^{121}A$ receptors displayed slightly lower potency than WT. These data are consistent with different receptor binding requirements for the amphiphilic orthosteric agonist, S1P, and the hydrophobic selective agonist, CYM-5442.

W146 has proved to be a reliable chiral-selective $S1P_1$ antagonist in vitro and in vivo (Sanna et al., 2006; Gonzalez-Cabrera et al., 2007; Yoon et al., 2008). As mentioned above, W146 antagonism of p42/p44 MAPK activity in these studies revealed two modes of action, competitive for S1P and non-competitive for CYM-5442. W146 antagonism of $S1P_1$ signal-

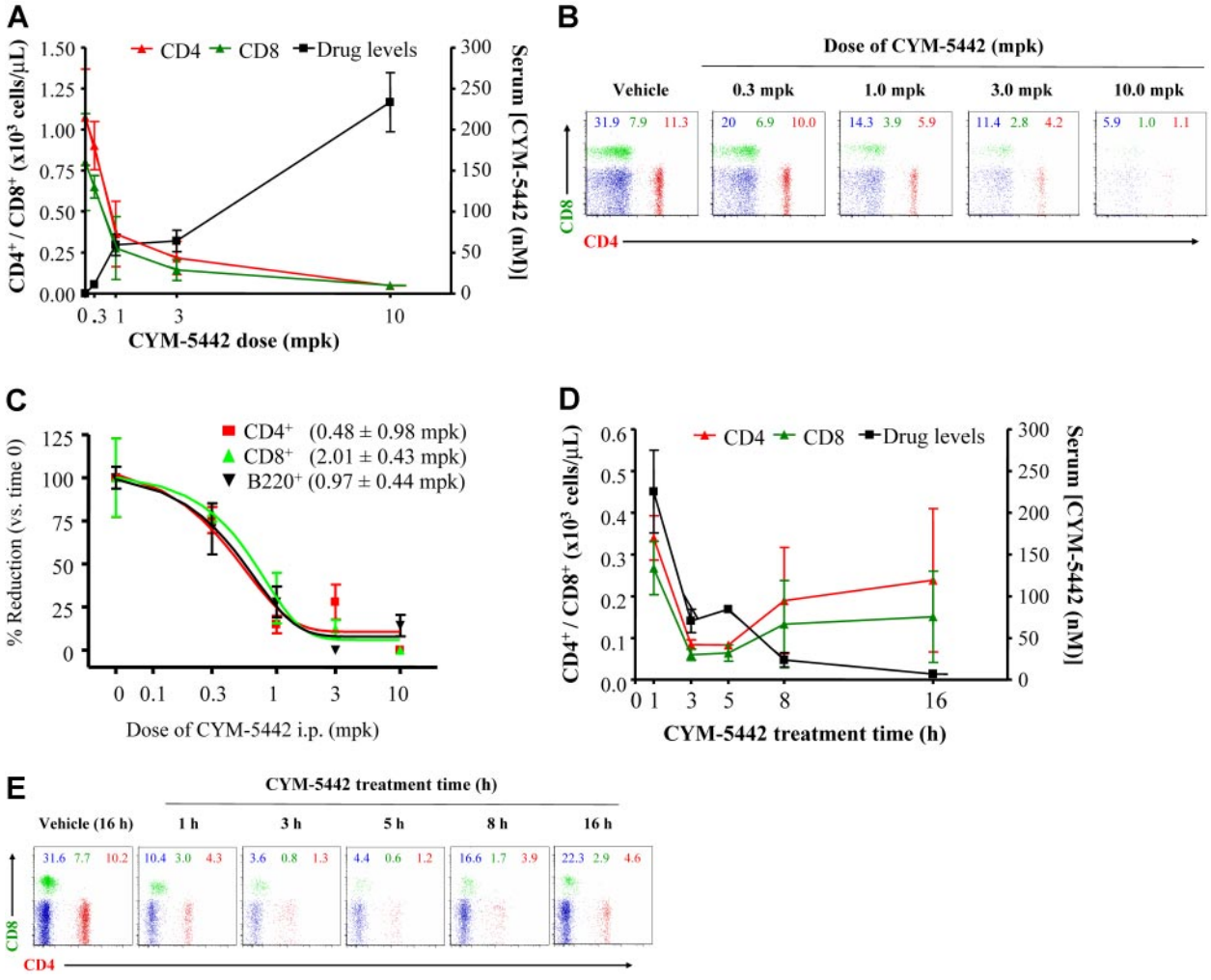

Fig. 6. CYM-5442 induction of lymphopenia in mice is dose- and time-dependent. C57BL/6J male mice (three mice for group) were injected intraperitoneally with either increasing doses of CYM-5442 or vehicle (water) to determine the dose dependence of CYM-5442 for induction of lymphopenia, or with a fixed dose (10 mg/kg) of CYM-5442 or vehicle for time course studies. For these studies, blood was extracted from each animal and used to measure $B220^+$, $CD4^+$, and $CD8^+$ cell counts, as well as CYM-5442 serum concentration. A, the average inhibition of single-positive CD4 ($CD4^+$, red) and CD8 ($CD8^+$, green) T-cell number is shown at the indicated dose of CYM-5442. The mean serum CYM-5442 concentration reveals that a 50 to 100 nM free CYM-5442 concentration range is required for induction of lymphopenia at 5 h. B, representative plots of $B220^+$ (blue), $CD4^+$ (red), and $CD8^+$ (green) percentage decreases are shown at the indicated CYM-5442 dose. C, the mean dose-response for CYM-5442 mediated inhibition of $B220^+$, $CD4^+$, and $CD8^+$ cell counts was used to calculate the ED_{50}s. D, time course of inhibition of $CD4^+$ and $CD8^+$ T-cell number after 10 mg/kg CYM-5442. The mean CYM-5442 serum concentration is also plotted. E, characteristic scatter plots of CYM-5442% inhibition of B-cell ($B\text{-}220^+$, blue) and T-cell ($CD4^+$, red and $CD8^+$, green) numbers are shown after 1, 3, 5, 8, and 16 h post CYM-5442 administration.

ing is therefore independent of whether S1P$_1$ activation is occurring through the orthosteric site or an adjacent hydrophobic site. Evidence for the spatial proximity of the orthosteric pocket to the hydrophobic one is provided by the competitive antagonist shift of W146 in the R^{120}A or E^{121}A mutated receptors in response to activation by CYM-5442. Because W146 is an amino-phosphonate, capable of making Arg and Glu headgroup interactions, these data suggest that W146 is no longer constrained in the single-point mutants thus allowing more flexible binding within the hydrophobic pocket. Consistent with these data, noncompetitive inhibition of CYM-5442 function was also observed with W146 in U2OS cells coupled to Tango S1P$_1$-bla, whereas W146 in the same assay was a competitive inhibitor against S1P (not shown). Other S1P$_1$ selective agonists with similar structures to CYM-5442 also display noncompetitive W146 inhibition (not shown), suggesting that diaryl-oxadiazole agonists such as CYM-5442 interact with a common hydrophobic pocket on S1P$_1$ (Schurer et al., 2008).

The in vivo data with CYM-5442 demonstrates its usefulness for inducing and maintaining S1P$_1$-dependent lymphopenia, with a minimal serum concentration for achieving maximal lymphopenia of approximately 50 nM. Because systemic S1P$_1$ antagonism with W146 reversed CYM-5442-induced lymphopenia, and W146 alone had no effect on B- and T-cell counts, the data indicate that S1P$_1$ agonist signals are minimal and obligatory for lymphopenia induction. These data provide additional evidence against the functional antagonism hypothesis for S1P$_1$-mediated immunomodulation (Matloubian et al., 2004; Schwab and Cyster, 2007).

All effects of CYM-5442, both in vitro and in vivo, are reversed or abolished by the selective S1P$_1$ receptor antagonist W146. These data restrict the pharmacological effects of CYM-5442 to this single receptor subtype. Although CYM-5442 is an enantiomeric mixture of 2 isomers, this mixture does not seem to contribute to the pharmacology or selectivity based upon our selective antagonist studies. Work is still ongoing to resolve the enantiomers. Differential crystallization using chiral salt forms such as L-tartaric acid have thus far been unsuccessful. Separation using chiral columns by HPLC is currently ongoing with no positive results yet and an enantiospecific synthesis may be formally required.

CYM-5442 possesses additional properties that make it a useful S1P$_1$ chemical agonist. CYM-5442 was found to be 10,000-fold selective for S1P$_1$ over S1P$_5$. Besides selectivity, CYM-5442 is approximately 10- to 50-fold more potent than SEW2871 in vitro, depending on which agonist format was used, and induces lymphopenia at approximately 5- to 10-fold lower doses than SEW2871. Favorable pharmacokinetics and moderate water solubility would make CYM-5442 a useful tool for studying S1P$_1$ function in tissues in which drug formulation or penetrance may present challenges (i.e., lung and central nervous system). The levels of CYM-5442 in brain tissue, with a brain-plasma ratio of 13:1 after a bolus dose in mice, are notable. The beneficial effects of FTY720 in ameliorating MS symptoms have been associated, in part, with the inhibition of BBB permeability occurring during disease progression. Central nervous system-penetrant and efficacious nonprodrug S1P$_1$ agonists such as CYM-5442, that are also antagonist reversible in the periphery, may be good proof-of-concept chemical tools for investigating the contributions of S1P$_1$ to MS therapy. These allow the contributions of BBB integrity, lymphocyte sequestration, and glial and neuronal S1P$_1$ function to be assessed. Indeed, selective S1P$_1$ agonists and antagonists have shown to inversely modulate the integrity of endothelial barriers in vivo (Sanna et al., 2006; Foss et al., 2007). We have data indicating that endothelial integrity is tonically regulated by the S1P-S1P$_1$ axis (Sanna et al., 2006). This servo mechanism results in agonist enhancement of barrier function by inhibiting leakage induced by proangiogenic stimuli, including vascular endothelial growth factor and thrombin. Antagonism alone leads to barrier-opening effects. These actions have been well documented in lung and skin vasculature, and having a matched agonist-antagonist pair such as CYM-5442 and W146 would be optimal for further studying the hypothetical endothelial S1P-S1P$_1$ rheostat.

Highly selective and potent chemical tools in general have characteristically slow off-rates and have been of great interest in recent crystallographic studies (Cherezov et al., 2007; Rosenbaum et al., 2007) to define both orthosteric and spatially distinct hydrophobic binding pockets within this family of class A GPCRs and the minimalist changes in receptor structure necessary for full pharmacological efficacy. Such chemical tools, when deeply characterized and broadly available to the field (Rosen et al., 2008), can affect the progress of mechanistic understanding in physiology, pathology, structural biology, and, ultimately, therapeutics.

TABLE 5

Lymphopenia by CYM-5442 administration is S1P$_1$-dependent

Mice (three per group) were first injected with a 20 mg/kg i.p. W146 in a 300-μl volume. W146 vehicle control mice received equal volume of 10 mM sodium carbonate/2% β-cyclodextrin (v/v). Thirty minutes later, animals were injected with either 2 mg/kg CYM-5442 or vehicle (sterile water). Five hours after CYM-5442 treatment, animals were euthanized and blood was collected into tubes containing EDTA. The number of B220-positive cells (B220$^+$, a marker for B cells) and single-positive CD4 (CD4$^+$) and CD8 (CD8$^+$) T cells was determined by FACS analysis and expressed as a percentage change relative to values obtained in animals receiving both drug vehicles. A sample aliquot of the blood was used to measure the serum drug concentration levels by LC-tandem mass spectrometry. Drug concentrations are included in parentheses as mean ± S.D.).

	W146 alone (1.75 ± 0.56 μM)	CYM-5442 (0.18 ± 0.05 μM)	W146 + CYM-5442 (1.76 ± 0.31 μM) (0.19 ± 0.04 μM)
B220$^+$	114.7 ± 5.9	46.0 ± 18.1*	92.4 ± 31.2
CD4$^+$	108.1 ± 17.4	53.5 ± 6.5*	89.1 ± 18.7
CD8$^+$	112.2 ± 19.6	47.4 ± 7.5*	92.2 ± 15.1

* $P < 0.05$ relative to W146 alone.

Acknowledgments

We are grateful to Bill Webb (Ctr. for Mass Spectrometry, TSRI) for measuring serum drug levels and Aaron Semana for expert technical assistance.

References

Ahmad M, Long JS, Pyne NJ, and Pyne S (2006) The effect of hypoxia on lipid phosphate receptor and sphingosine kinase expression and mitogen-activated protein kinase signaling in human pulmonary smooth muscle cells. *Prostaglandins Other Lipid Mediat* **79:**278–286.

Alfonso C, McHeyzer-Williams MG, and Rosen H (2006) CD69 down-modulation and inhibition of thymic egress by short and long-term selective chemical agonism of S1P1 receptors. *Eur J Immunol* **36:**149–159.

Balatoni B, Storch MK, Swoboda EM, Schönborn V, Koziel A, Lambrou GN, Hiestand PC, Weissert R, and Foster CA (2007) FTY720 sustains and restores neuronal function in the DA rat model of MOG-induced experimental autoimmune encephalomyelitis. *Brain Res Bull* **74:**307–316.

Cherezov V, Rosenbaum DM, Hanson MA, Rasmussen SG, Thian FS, Kobilka TS, Choi HJ, Kuhn P, Weis WI, Kobilka BK, et al. (2007) High-resolution crystal structure of an engineered human beta2-adrenergic G protein-coupled receptor. *Science* **318:**1258–1265.

Dudek SM, Jacobson JR, Chiang ET, Birukov KG, Wang P, Zhan X, and Garcia JG (2004) Pulmonary endothelial cell barrier enhancement by sphingosine 1-phos-

phate: roles for cortactin and myosin light chain kinase. *J Biol Chem* **279:**24692–24700.
Foss FW Jr, Snyder AH, Davis MD, Rouse M, Okusa MD, Lynch KR, and Macdonald TL (2007) Synthesis and biological evaluation of gamma-aminophosphonates as potent, subtype-selective sphingosine 1-phosphate receptor agonists and antagonists. *Bioorg Med Chem* **15:**663–677.
Foster CA, Mechtcheriakova D, Storch MK, Balatoni B, Howard LM, Bornancin F, Wlachos A, Sobanov J, Kinnunen A and Baumruker T (2008) FTY720 rescue therapy in the dark agouti rat model of experimental autoimmune encephalomyelitis: expression of central nervous system genes and reversal of blood-brain-barrier damage. *Brain Pathology*, in press.
Fujiwara Y, Osborne DA, Walker MD, Wang DA, Bautista DA, Liliom K, Van Brocklyn JR, Parrill AL, and Tigyi G (2007) Identification of the hydrophobic ligand binding pocket of the $S1P_1$ receptor. *J Biol Chem* **282:**2374–2385.
Gonzalez-Cabrera PJ, Hla T, and Rosen H (2007) Mapping pathways downstream of sphingosine 1-phosphate subtype 1 by differential chemical perturbation and proteomics. *J Biol Chem* **282:**7254–7264.
Hiestand PC, Rausch M, Meier DP, and Foster CA (2008) Ascomycete derivative to MS therapeutic: S1P receptor modulator FTY720. *Prog Drug Res* **66:**361, 363–381.
Jo E, Sanna MG, Gonzalez-Cabrera PJ, Thangada S, Tigyi G, Osborne DA, Hla T, Parrill AL, and Rosen H (2005) S1P1-Selective in vivo-active agonists from high-throughput screening: off-the-shelf chemical probes of receptor interactions, signaling, and fate. *Chem Biol* **12:**703–715.
Kataoka H, Sugahara K, Shimano K, Teshima K, Koyama M, Fukunari A, and Chiba K (2005) FTY720, sphingosine 1-phosphate receptor modulator, ameliorates experimental autoimmune encephalomyelitis by inhibition of T cell infiltration. *Cell Mol Immunol* **2:**439–448.
Lee MJ, Thangada S, Claffey KP, Ancellin N, Liu CH, Kluk M, Volpi M, Sha'afi RI, and Hla T (1999) Vascular endothelial cell adherens junction assembly and morphogenesis induced by sphingosine-1-phosphate. *Cell* **99:**301–312.
Liu CH, Thangada S, Lee MJ, Van Brocklyn JR, Spiegel S, and Hla T (1999) Ligand-induced trafficking of the sphingosine-1-phosphate receptor EDG-1. *Mol Biol Cell* **10:**1179–1190.
Mandala S, Hajdu R, Bergstrom J, Quackenbush E, Xie J, Milligan J, Thornton R, Shei GJ, Card D, Keohane C, et al. (2002) Alteration of lymphocyte trafficking by sphingosine-1-phosphate receptor agonists. *Science* **296:**346–349.
Miron VE, Schubart A, and Antel JP (2008) Central nervous system-directed effects of FTY720 (fingolimod) *J Neurol Sci*, in press.
Matloubian M, Lo CG, Cinamon G, Lesneski MJ, Xu Y, Brinkmann V, Allende ML, Proia RL, and Cyster JG (2004) Lymphocyte egress from thymus and peripheral lymphoid organs is dependent on S1P receptor 1. *Nature* **427:**355–360.
Oo ML, Thangada S, Wu MT, Liu CH, Macdonald TL, Lynch KR, Lin CY, and Hla T (2007) Immunosuppressive and anti-angiogenic sphingosine 1-phosphate receptor-1 agonists induce ubiquitinylation and proteasomal degradation of the receptor. *J Biol Chem* **282:**9082–9089.
Parrill AL, Wang D, Bautista DL, Van Brocklyn JR, Lorincz Z, Fischer DJ, Baker DL, Liliom K, Spiegel S, and Tigyi G (2000) Identification of Edg1 receptor residues that recognize sphingosine 1-phosphate. *J Biol Chem* **275:**39379–39384.
Rosen H, Alfonso C, Surh CD, and McHeyzer-Williams MG (2003) Rapid induction of medullary thymocyte phenotypic maturation and egress inhibition by nanomolar sphingosine 1-phosphate receptor agonist. *Proc Natl Acad Sci* **100:**10907–10912.
Rosen H and Goetzl EJ (2005) Sphingosine 1-phosphate and its receptors: An autocrine and paracrine network. *Nat Rev Immunol* **5:**560–570.
Rosen H, Gonzalez-Cabrera P, Marsolais D, Cahalan S, Don AS, and Sanna MG (2008) Modulating tone: the overture of S1P receptor immunotherapeutics. *Immunol Rev* **223:**221–235.
Rosen H, Sanna MG, Cahalan SM, and Gonzalez-Cabrera PJ (2007) Tipping the gatekeeper: S1P regulation of endothelial barrier function. *Trends Immunol* **28:**102–107.
Rosenbaum DM, Cherezov V, Hanson MA, Rasmussen SG, Thian FS, Kobilka TS, Choi HJ, Yao XJ, Weis WI, Stevens RC, et al. (2007) GPCR engineering yields high-resolution structural insights into beta2-adrenergic receptor function. *Science* **318:**1266–1273.
Sanna MG, Liao J, Jo E, Alfonso C, Ahn MY, Peterson MS, Webb B, Lefebvre S, Chun J, Gray N, et al. (2004) Sphingosine 1-phosphate (S1P) receptor subtypes S1P1 and S1P3, respectively, regulate lymphocyte recirculation and heart rate. *J Biol Chem* **279:**13839–13848.
Sanna MG, Wang SK, Gonzalez-Cabrera PJ, Don A, Marsolais D, Matheu MP, Wei SH, Parker I, Jo E, Cheng WC, et al. (2006) Enhancement of capillary leakage and restoration of lymphocyte egress by a chiral S1P1 antagonist in vivo. *Nat Chem Biol* **2:**434–441.
Sanchez T, Estrada-Hernandez T, Paik JH, Wu MT, Venkataraman K, Brinkmann V, Claffey K, and Hla T (2003) Phosphorylation and action of the immunomodulator FTY720 inhibits vascular endothelial cell growth factor-induced vascular permeability. *J Biol Chem* **278:**47281–47290.
Schürer SC, Brown SJ, Gonzalez-Cabrera PJ, Schaeffer MT, Chapman J, Jo E, Chase P, Spicer T, Hodder P, and Rosen H (2008) Ligand-binding pocket shape differences between sphingosine 1-phosphate (S1P) receptors S1P1 and S1P3 determine efficiency of chemical probe identification by ultrahigh-throughput screening. *ACS Chem Biol* **3:**486–498.
Schwab SR and Cyster JG (2007) Finding a way out: lymphocyte egress from lymphoid organs. *Nat Immunol* **8:**1295–1301.
Sorensen SD, Nicole O, Peavy RD, Montoya LM, Lee CJ, Murphy TJ, Traynelis SF, and Hepler JR (2003) Common signaling pathways link activation of murine PAR-1, LPA, and S1P receptors to proliferation of astrocytes. *Mol Pharmacol* **64:**1199–1209.
Wang DA, Lorincz Z, Bautista DL, Liliom K, Tigyi G, and Parrill AL (2001) A single amino acid determines lysophospholipid specificity of the S1P1 (EDG1) and LPA1 (EDG2) phospholipid growth factor receptors. *J Biol Chem* **276:**49213–49220.
Wei SH, Rosen H, Matheu MP, Sanna MG, Wang SK, Jo E, Wong CH, Parker I, and Cahalan MD (2005) Sphingosine 1-phosphate type 1 receptor agonism inhibits transendothelial migration of medullary T cells to lymphatic sinuses. *Nat Immunol* **6:**1228–1235.
Weinreich MA and Hogquist KA (2008) Thymic emigration: when and how T cells leave home. *J Immunol* **181:**2265–2270.
Yoon CM, Hong BS, Moon HG, Lim S, Suh PG, Kim YK, Chae CB, and Gho YS (2008) Sphingosine-1-phosphate promotes lymphangiogenesis by stimulating $S1P1/G_i/PLC/Ca^{2+}$ signaling pathways. *Blood* **112:**1129–1138.

Address correspondence to: Hugh Rosen, 10550 North Torrey Pines Rd, ICND-118, La Jolla, CA 92037. E-mail: hrosen@scripps.edu